Blended-record imaging: investigations on optimization and possible applications

Daniel Carvalho Rocha Junior, CPGG/UFBA and Paul Sava, Center for Wave Phenomena

Copyright 2013, SBGf - Sociedade Brasileira de Geofísica.

This paper was prepared for presentation at the 13th International Congress of the Brazilian Geophysical Society, held in Rio de Janeiro, Brazil, August 26-29, 2013.

Contents of this paper were reviewed by the Technical Committee of the 13th International Congress of The Brazilian Geophysical Society and do not necessarily represent any position of the SBGf, its officers or members. Electronic reproduction or storage of any part of this paper for commercial purposes without the written consent of The Brazilian Geophysical Society is prohibited.

Abstract

Blended-record imaging allows us in principle to reduce the imaging computational cost by processing more than one record at a time. The main drawback of blended-record imaging is that wavefields corresponding to different experiments interact with one another, producing fake reflectors – an effect know as imaging cross-talk. Different strategies can be employed to attenuate the artifacts, including filtering in extended images, or filtering collections of images obtained for different combinations of blended records, as discussed in this paper. We conclude that if the velocity used for imaging is correct, simple stacking provides an effective cross-talk attenuation procedure. However, this strategy is not applicable when the model is inaccurate and image-domain shot gathers are characterized by moveout. More advanced filtering is necessary in this situation in order to clean-up the image gathers and prepare them for migration velocity analysis.

Introduction

Seismic industry has taken significant effort to image complex geologic structures by collecting large amounts of data, generally redundant, in order to achieve high level of precision and large signal to noise ratio. Recent trends show that data volumes continue to grow, in particular due to the development of wide-azimuth data acquisition. The increased data volume lead to improved subsurface imaging and more effective noise suppression (multiples, in particular), but this improvement in imaging quality comes at the expense of growing computational cost.

One possible strategy to reduce the computational cost is to process collections of shot records, a strategy known by the name of blended-record imaging (Sava, 2007; Poole and others, 2010; Biondi, 2007). Although effective in reducing computational cost, blended-record imaging is hampered by image artifacts due to the interference among wavefields characterizing different seismic experiments, i.e. different shots. These cross-talk artifacts resemble real reflectors and interfere with the geology, thus hampering interpretation.

Imaging computational cost is proportional to number of migrations applied, therefore we can write:

$$C_s^t = N_s C_m \tag{1}$$

and

$$C_e^t = N_e C_m \tag{2}$$

where C_m is the cost of migration, C_s^t and C_e^t are the total cost of shot-record and blended-record imaging, respectively, and N_s and N_e are the number of separate migrations performed for shot-record and for blended-record imaging. Ideally, the number of blended-record migrations should be significantly smaller than the number of shot-record migrations ($N_e << N_s$) (Godwin and Sava, 2010).

As indicated earlier, the cross-talk artifacts are related to the cross-correlations between source and receiver wavefields pertaining to different sources. For wave-equation migration, the cross-correlation imaging condition can be written as (Claerbout, 1985)

$$I(\mathbf{x}) = \sum_k \int \overline{s_k(\mathbf{x},\omega)} r_k(\mathbf{x},\omega) d\omega + \sum_{k\neq j} \int \overline{s_k(\mathbf{x},\omega)} r_j(\mathbf{x},\omega) d\omega \tag{3}$$

where the first term correspond to the image we seek, and the second term corresponds to the cross-talk (Perrone and Sava, 2009). The condition $k \neq j$ in the second term indicates summation over different experiments.

In following sections, we investigate the cross-talk characterizing blended-record imaging and address several questions relevant for interpretation of wave-equation images: How do the artifacts look in extended images and how do they impact image quality? What filtering can be employed to attenuate cross-talk artifacts and how does this impact migration velocity analysis?

Extended imaging condition

In wavefield extrapolation imaging, reflectors exist where source and receiver wavefields match. This principle is the core of conventional imaging condition (CIC), and mathematically it means that the image is formed at zero-lag of the temporal cross-correlation between source and receiver wavefields (Sava and Fomel, 2006). The zero-lag image is the only output of this process, although correlation can give information for all time-lags between the source and receiver wavefields which depend on space $\mathbf{x}$ and frequency ω.

In order to achieve more information from wavefield correlation related to acquisition or illumination parameters, angle of incidence, among others, we can apply an extended imaging condition (EIC). Mathematically, this simply implies that we preserve in the output image the space and time-lags of the cross-correlation:

$$\begin{aligned} I(\mathbf{x},\lambda,\tau) = &\sum_k \int e^{2i\omega\tau} \overline{s_k(\mathbf{x}-\lambda,\omega)} r_k(\mathbf{x}+\lambda,\omega) d\omega \\ &+ \sum_{k\neq j} \int e^{2i\omega\tau} \overline{s_k(\mathbf{x}-\lambda,\omega)} r_j(\mathbf{x}+\lambda,\omega) d\omega \end{aligned} \tag{4}$$

Information from images obtained by the EIC is generally displayed in two forms: Common Image Point Gathers (CIP) or Common Image Gathers (CIG). The first one displays all lags configurations (τ, λ) for a point in space, and the second option displays $\tau, \lambda_x, \lambda_y$ for a fixed horizontal position. An angle decomposition, i.e. reflection information content corresponding to incidence angles, can also be applied on CIGs, thus generating representations of reflectivity as a function of reflection angles z, θ, ϕ. More information about EICs and their angle decomposition can be found in the literature (Sava and Fomel, 2003; Rickett and Sava, 2002; Sava and Vasconcelos, 2011).

Figures 1 and 2 illustrate the behavior of CIP and CIG extended images obtained with blended record imaging. In these examples, we consider three shots imaged simultaneously by wave-equation migration. In CIPs, true reflections go through the origin of the lag coordinate system. All other events are cross-talk. Similarly, in CIGs, the true events intersect at the origin of the space- and time-lag axes. This behavior indicates that we have, in principle, enough information to attenuate these cross-talk artifacts since this behavior differs significantly from the behavior of the true reflections

Blended-record image quality optimization

Stacking over experiments in blended-records is a simple and mostly efficient way to diminish cross-talk artifacts that are very strong on experiments individually. It can be considered as an averaging of image at each experiment, and this averaging operation is similar to taking the DC component of a collection of images in the Fourier domain. This is physically reasonable, since true reflectors are always in the same location regardless of experiment, whereas artifacts like cross-talk are incoherent over experiments.

Using the coherency of true events as a function of experiments, and the fact that stacking is a simple Fourier-domain filter, we can investigate other similar filters for blended-record images. We can group the images corresponding to different experiments and filter them in the "experiment" domain, similarly to the process implemented by the simple summation discussed earlier.

For example, an experiment gather is shown in Figure 4 for a model with several reflectors (Fig. 3). In Figure 4(a), we can clearly see the difference in frequency spectrum between true reflections (DC component) and cross-talk (higher wave-numbers). In this case, the wavenumber refers to the Fourier domain pair of the experiment axis shown in Figure 4(b). Cross-talk artifacts appear at high wave-numbers, but reflections are strong at low-frequency, which confirms the idea of reflectors staying spatially fixed over experiments. These figures also explain why stacking improves blended image quality, since only DC component is preserved during stacking.

Using these observations, we can consider alternative low-pass filters to attenuate the cross-talk artifacts. Figures 5(b) and 5(c), show the expression of a low-pass filter and of a SVD filter, respectively. Both filters enhance the coherent events, although the SVD filter seems to be more reliable in preserving the character of the original experiment gather.

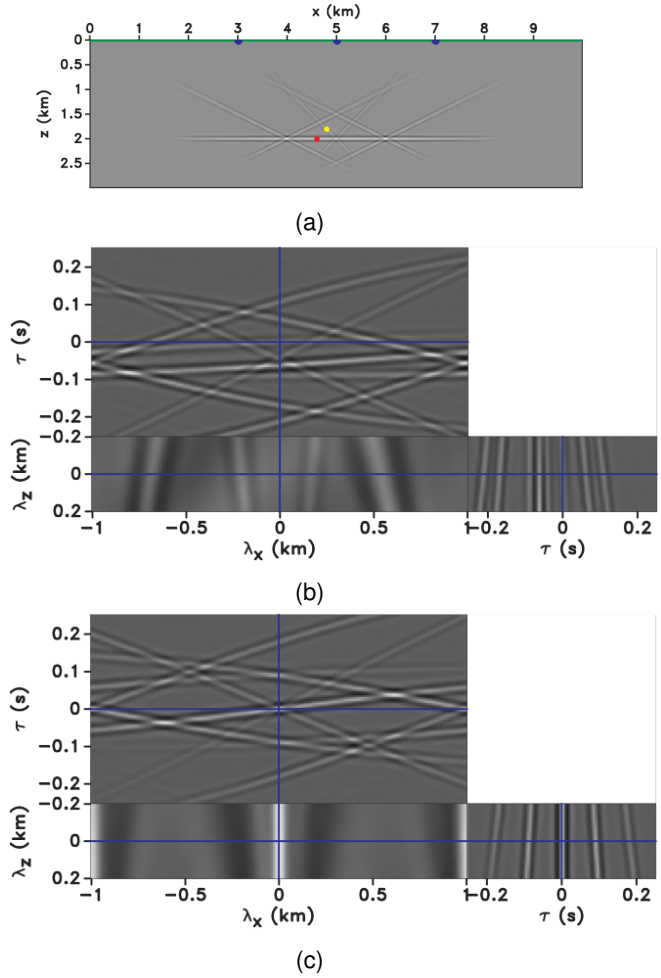

Figure 1: (a) Image obtained for a model with one reflector 2 km depth. The red and yellow dots show the locations of two CIPs. (b) A CIP away from the reflector (yellow dot). (c) A CIP on the reflector (red dot).

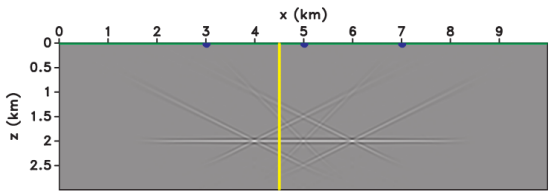

(a)

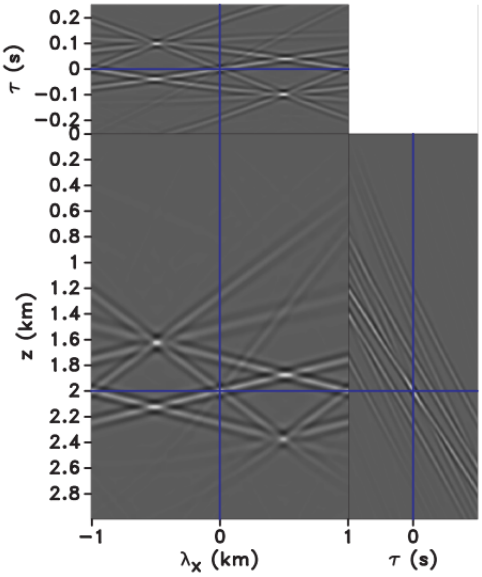

(b)

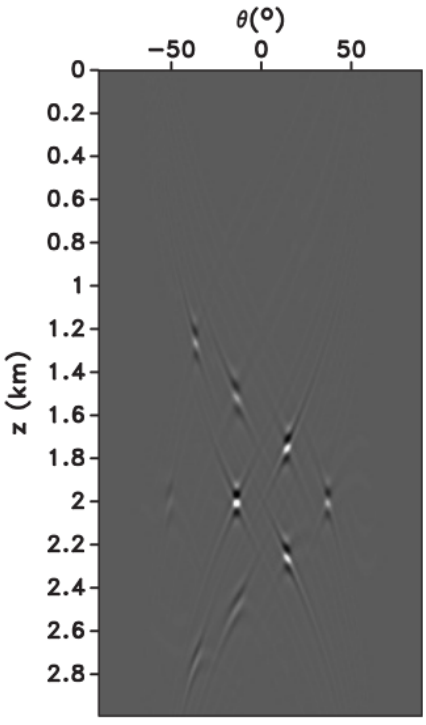

(c)

Figure 2: (a) Image obtained for a model with one reflector 2 km depth. The yellow line shows the location of a CIG. (b) The extended CIG at the location of the yellow line, (c) and its angle decomposition.

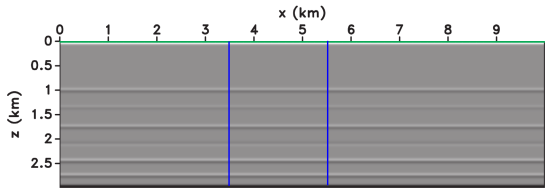

Figure 3: Model used to generate results in Figures 4 and 5. Blue lines show locations of experiments gathers investigated, at x=3.5 km (Figure 5) and x=5.5 km (Figure 4).

Reflectors are enhanced after experiment-domain filtering, as seen in Figures 5(b) and 5(c). Although the experiment gathers are different from one-another, stacking applied on these filtered experiment gathers look similar to stacking without filtering, as it can be seen in Figures 5(d), 5(e) and 5(f). We conclude the filtering is necessary to attenuate cross-talk artifacts in experiment gathers, but this filtering does not improve significantly the stack over experiments, i.e. the image. Nevertheless, for migration velocity analysis we need to work with the image before stacking over experiments, so filtering is necessary to understand the moveout of the gathers. Furthermore, when velocity is incorrect, stacking cannot by itself attenuate the cross-talk artifacts.

Blended-record migration velocity analysis

MVA using shot-record imaging has a large cost, since a considerable number of shot-record migrations are necessary at each iteration for a given model. A high quality image is mostly needed for the final migration, but not for intermediate migrations taken during MVA. Assuming this, blended-record imaging could be used as a method to reduce cost during MVA iterations.

Figure 6 shows a different migration velocity used to test shot-record and blended-record imaging. The model contains a Gaussian low-velocity anomaly and a reflector. Data contains 40 shot gathers with sources spacing 20 meters from each other. For shot-record imaging, we run 40 migrations, with correct and incorrect velocities For blended-record imaging, we run 5 migrations with 8 simultaneous sources using correct and incorrect velocities.

Results show that incorrect velocity affects more blended-record migration than shot-record migration. The cross-talk artifacts increase substantially, especially nearby the low-velocity zone. This indicates that simple stacking is not sufficient to attenuate the cross-talk noise, as needed for velocity analysis. Although stacking was sufficient for imaging with correct velocity, more sophisticated filtering methods are necessary to clean experiment gathers before they can be used for migration velocity analysis.

Conclusions

Blended-record imaging has the potential to reduce significantly the computational cost of wave-equation migration, especially during migration velocity analysis iterations. However, blended-record images are impacted

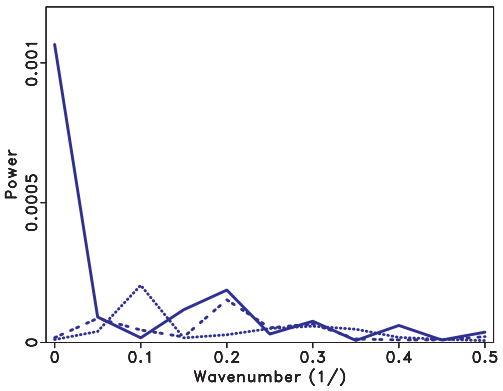

(a)

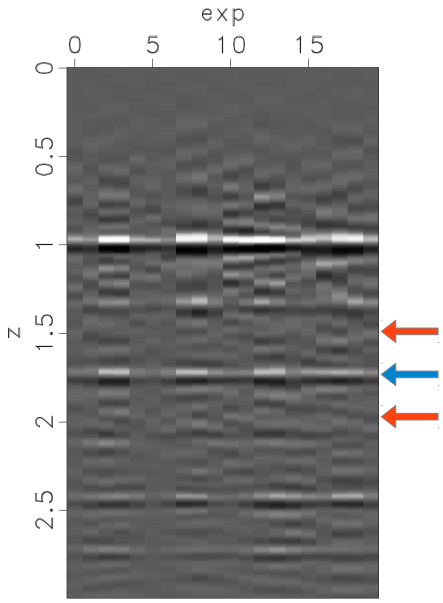

(b)

Figure 4: (a) Frequency spectrum as a function of experiment: on a reflector (solid line), and away from a reflector (dashed lines). (b) Experiment gather at x=5.5 km used in (a); arrows pointing where frequency plots are taken: on reflector (blue arrow) and away from a reflector (red arrows).

by cross-talk artifacts which may obstruct reflectors corresponding to the true geologic structure. Cross-talk artifacts are different from true reflections when imaging is performed using extended images. This conclusion is true both in space-lag gathers, as well as in angle gathers.

Cross-talk can be attenuated by many techniques, although for the case of imaging with correct velocity, simple stacking appears to be one of the most effective techniques. However, when the imaging velocity is incorrect, stacking does not eliminate cross-talk and more sophisticated techniques are necessary.

References

Biondi, B. L., 2007, Concepts and applications in 3d seismic imaging: SEG - EAGE.

Claerbout, J. F., 1985, Imaging the earth's interior: Blackwell Scientific Publications.

Godwin, J., and Sava, P., 2010, Blended source imaging by amplitude encoding: 80th Annual International Meeting, SEG, Expanded Abstracts, 3125-3129.

Perrone, F., and Sava, P., 2009, Comparison of shot encoding functions for reverse-time migration: 79th Annual International Meeting, SEG, Expanded Abstracts, 2980-2984.

Poole, T., et al., 2010, Deconvolution imaging conditions and cross-talk suppression: Geophysics, **75**, no. 6, W1–W12.

Rickett, J., and Sava, P., 2002, Offset and angle-domain common image-point gathers for shot-profile migration: Geophysics, **67**, no. 3, 883–889.

Sava, P., and Fomel, S., 2003, Angle-domain common image gathers by wavefield continuation methods: Geophysics, **68**, no. 3, 1065–1074.

Sava, P., and Fomel, S., 2006, Generalized imaging condition for wave-equation migration: 68th Meeting, EAGE, Expanded Abstracts.

Sava, P., and Vasconcelos, I., 2011, Extended imaging conditions for wave-equation migration: Geophysical Prospecting, **59**, no. 1, 35–55.

Sava, P., 2007, Stereographic imaging condition for wave-equation migration: Geophysics, **72**, no. 6, A87–A91.

Tang, Y., and Biondi, B. L., 2009, Least-squares migration of blended data: 79th Annual International Meeting, SEG, Expanded Abstracts, 2859-2863.

Acknowledgments

The reproducible numeric examples in this paper use the Madagascar open-source software package freely available from http://www.ahay.org.

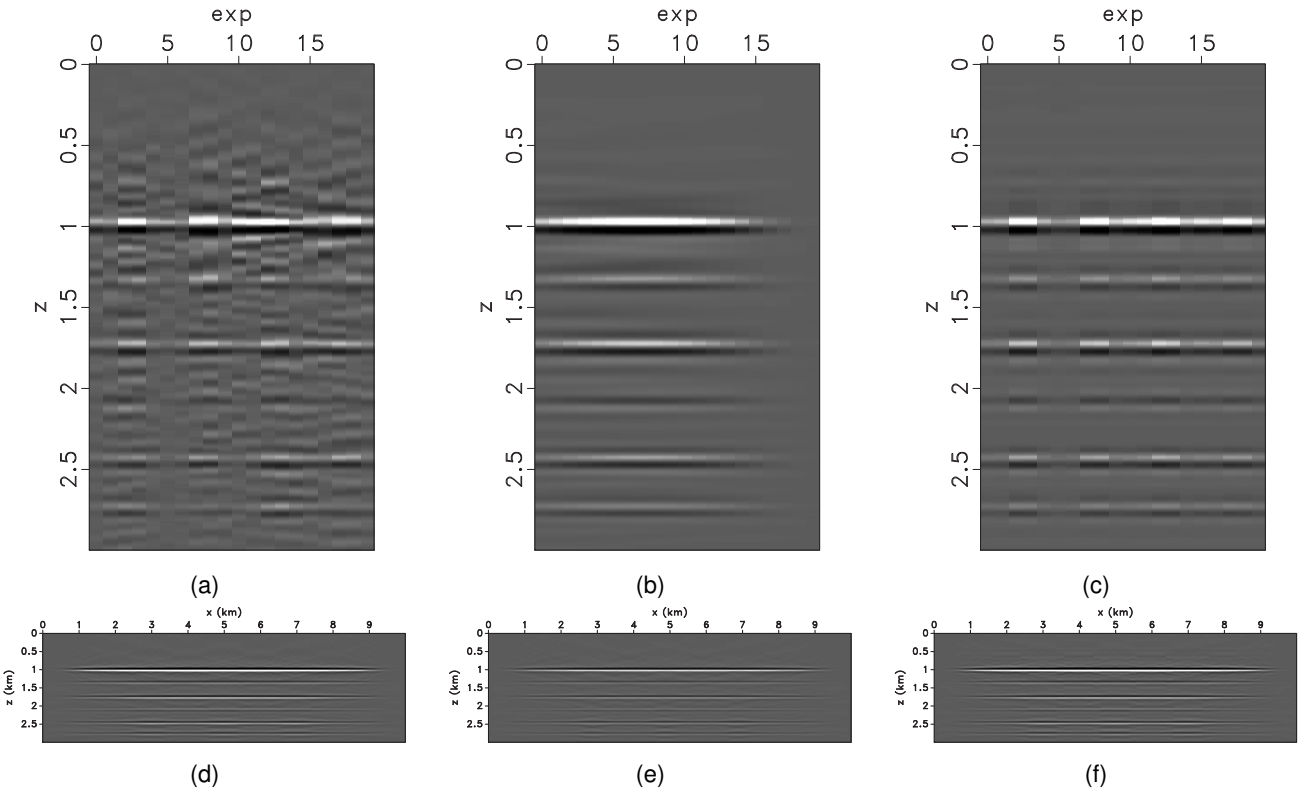

Figure 5: (a) Experiment gather at x=3.5 km and results for (b) a bandpass filter and (c) a SVD filter. Final images results for (d) plain stacking, (e) low-pass filtering and (f) SVD filtering over the experiment domain.

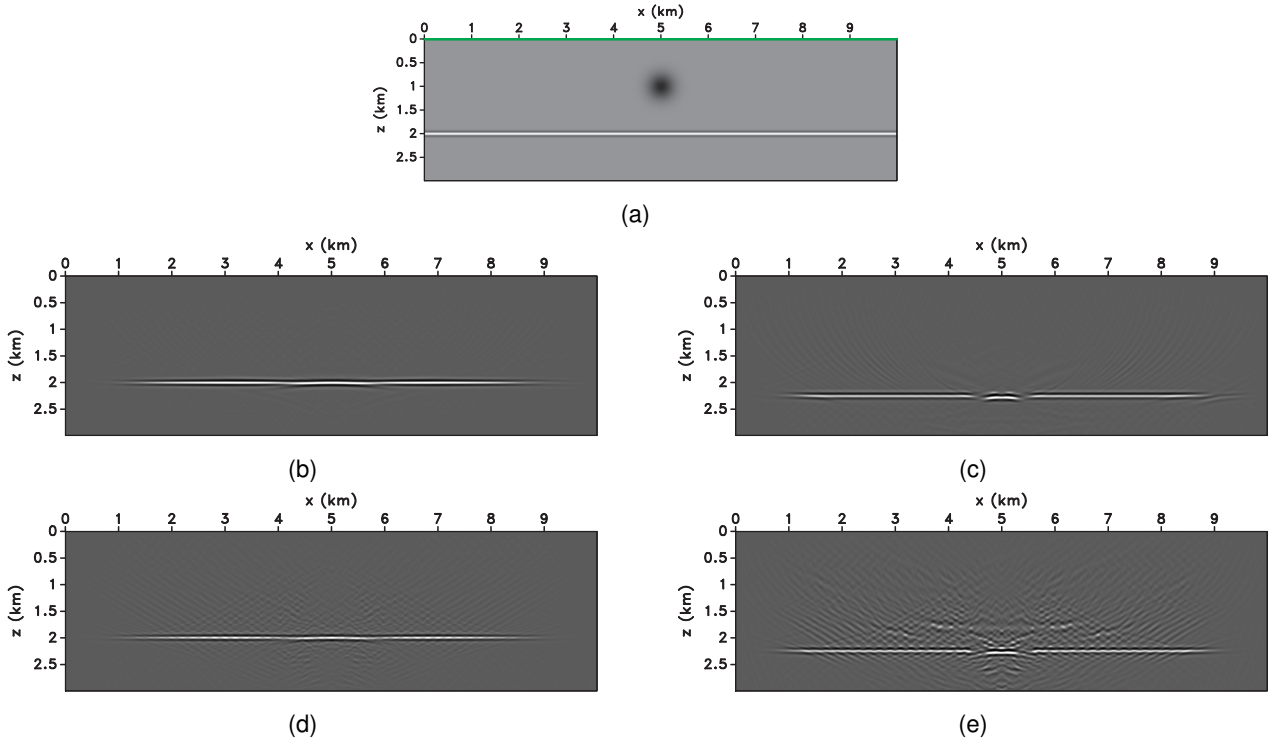

Figure 6: (a) Model used to test the impact of imaging with incorrect velocities. Shot-record migration with (b) correct velocity, and (c) with 12% increased velocity. Blended-record migration with (d) correct velocity, and (e) with 12% increased velocity.